Stochastic Dynamic Analysis of Marine Risers Considering Gaussian System Uncertainties

Pinghe Ni [1, 2], Jun Li [1,], Hong Hao [1], Yong Xia [2]*

[1]*Centre for Infrastructural Monitoring and Protection, School of Civil and Mechanical Engineering,*

Curtin University, Kent Street, Bentley, WA 6102, Australia

[2]*Department of Civil and Environmental Engineering, The Hong Kong Polytechnic University,*

Hung Hom, Kowloon, Hong Kong

Abstract: This paper performs the stochastic dynamic response analysis of marine risers with material uncertainties, i.e. in the mass density and elastic modulus, by using Stochastic Finite Element Method (SFEM) and model reduction technique. These uncertainties are assumed having Gaussian distributions. The random mass density and elastic modulus are represented by using the Karhunen–Loeve (KL) expansion. The Polynomial Chaos (PC) expansion is adopted to represent the vibration response because the covariance of the output is unknown. Model reduction based on the Iterated Improved Reduced System (IIRS) technique is applied to eliminate the PC coefficients of the slave degrees of freedom to reduce the dimension of the stochastic system. Monte Carlo Simulation (MCS) is conducted to obtain the reference response statistics. Two numerical examples are studied in this paper. The response statistics from the proposed approach are compared with those from MCS. It is noted that the computational time is significantly reduced while the accuracy is kept. The results demonstrate the efficiency of the proposed approach for stochastic dynamic response analysis of marine risers.

Keywords: Karhunen–Loeve Expansion; Polynomial Chaos expansion; Monte Carlo Simulation; Stochastic Finite Element Method; Model Reduction;

*Corresponding Author, Centre for Infrastructural Monitoring and Protection, School of Civil and Mechanical Engineering, Curtin University, Kent Street, Bentley, WA 6102, Australia. Email: junli@curtin.edu.au; LI.Jun@connect.polyu.hk, Tel.: +61 8 9266 5140; Fax: +61 8 9266 2681.

1 Introduction

Marine risers are used to connect the offshore platforms on the water surface to the well head at the sea floor, ensuring the safe operations of offshore platforms in the oil and gas industry. Excess vibration of risers is considered as the main cause of the fatigue induced degradation and failure [1], which could lead to catastrophic infrastructure damage and environmental consequence. Significant attention has been drawn to investigate the dynamic vibration analysis of marine risers. Lei et al. [2] proposed a frequency domain method to investigate the effect of time-dependent tension force on the lateral deflection of marine risers. Tsukada and Morooka [3] developed a numerical method to estimate the vortex-induced vibration forces of a catenary riser. Han et al. [4] carried out experimental tests to investigate the dynamic characteristics of vortex-induced vibrations of a riser. The dynamic response characteristics were obtained from the analysis of strain responses, displacement amplitudes, dominant modes, response frequencies and drag force coefficients. Rivero-Angeles et al. [5] presented a comparison study on the modal identification of offshore risers by using two methods, namely, the Frequency Domain Decomposition Method and the Conventional Spectral Analysis Method, with numerical simulation data. Gao et al. [6] proposed a method to study riser's fatigue damage induced by the vortex-induced vibrations. The riser was defined as a pinned-pinned cable model and the fatigue damage of the riser can be predicted by applying the modal superposition method combined with the S - N curve.

In the above-reviewed studies on the dynamic analysis, modal identification and damage detection of marine risers, deterministic analyses are conducted by assuming the system parameters with specific constant values. However, in reality, the inevitable random fluctuations in the structural system, i.e., random variations of the material properties including mass and stiffness, affect the structural responses, which have not been well considered. For example, the growing marine organisms have a number of adverse effects on offshore structures, one of which is that it may change the mass density of the risers significantly. Moreover, the long term corrosion in aggressive sea environment may also significantly affect the stiffness of risers. These effects should be properly considered for a better understanding of the lifetime performance of marine structures.

Stochastic Finite Element Method (SFEM) [7] has been successfully applied in many engineering areas, for example, structural analysis with uncertain system parameters [8], bridge–vehicle interaction analysis [9], elasto-plastic response analysis [10], etc. Some studies have been conducted to perform the stochastic dynamic analysis of offshore structures. Bi et al. [11] carried out the stochastic seismic response analysis of offshore pipelines subjected to spatially varying ground motions. The mean peak seismic responses of pipelines in the axial and lateral directions were stochastically formulated in the frequency domain. Foo et al. [12] performed the stochastic simulations of riser sections. Three-dimensional riser-sections undergoing elastic deformations due to random pressure loads were considered. The riser's deformations with the stochastic elastic modulus and deterministic loading were also studied. He and Low [13] predicted the probability of riser collision under stochastic excitations and various uncertainties. The considered random variables included the current, drag coefficient, vessel motions and riser mass, and the likelihood of collision was obtained. Mousavi et al. [14] estimated the probability of fatigue or strength failure of steel catenary risers. The uncertainties in the yield strength and fatigue capacities, as well as the environmental conditions, were considered. The proposed method was combined with the integrity based optimal design to improve the safety of steel catenary risers. Qiu et al. [15] discussed the uncertainties related to the prediction of loads and responses of ocean and offshore structures, particularly in the model tests. Uncertain parameters included the physical properties of the fluid, initial conditions, model definition, environment, scaling, instrumentation and human factors. Uncertainty effect on the dynamic response of offshore structural risers have not been well investigated yet.

This paper investigates the effect of uncertainties in the structural parameters, i.e. mass density and elastic modulus, on the dynamic responses of the marine risers under sea wave loads. The stochastic mass density and elastic modulus are represented by using Karhunen–Loeve (KL) expansion. The mean value and standard deviation are assumed based on design and available information, and the probability function of random parameters is assumed to follow the Gaussian distribution. Polynomial Chaos (PC) expansion is adopted to represent the stochastic output response, in which the covariance matrix of the output response is unknown. Two numerical examples are studied in this paper. In the first example, the marine riser is simulated as a beam structure. Then a more complicated

cylinder model with shell elements is studied in the second example. Model reduction based on the Iterated Improved Reduced System (IIRS) technique is applied to reduce the dimensions of stochastci system matrices and improve the computational efficiency. The response statistics of the modelled riser with and without using the model reduction technique are compared with those from Monte Carlo Simulation (MCS). Results demonstrate the accuracy and efficiency of the proposed approach. It should be noted that in reality the offshore environmental and loading conditions usually experience, if not more significant, the same random fluctuations as the structural parameters. They are, however, not considered in the present study because the primary objective of the present study is to introduce and demonstrate the accuracy and efficiency of the reduction method in stochastic analysis of dynamic structural responses. Without loss of generality, only the random variations of structural parameters are considered.

This paper is organized as follows. In Section 2, the theoretical background of KL expansion and PC expansion for representing the random processes is briefly reviewed. KL expansion can be used to represent the known stochastic fields (i.e., the stochastic inputs) efficiently. PC expansion is adopted to represent the stochastic outputs since the covariance matrix of the random output is unknown. In Section 3, the deterministic equation of motion of an offshore riser is introduced first. The random fields of the mass density and elastic modulus are generated by using KL expansions, and random output responses are represented with PC expansions. The stochastic dynamic system is formulated in Section 3.3. Model reduction technique is then used to reduce the dimensions of the stochastic dynamic system in the response analysis by eliminating the unfavorable degrees-of-freedom (DOFs). Numerical examples and simulation results are described and discussed in Section 4, and then the conclusions are given in Section 5.

2 Representation of stochastic processes

2.1 KL expansion

The theoretical background of KL expansion [16] will be briefly reviewed herein for the completeness of this paper. Let $H(\chi, \theta)$ be a second-order random process, which is a function of

the position vector defined over the domain V, belonging to the space of random events Ω. $\bar{H}(\chi)$ is denoted as the mathematical expectation of $H(\chi,\theta)$ over all possible realizations of the process, and $C_{\text{cov}}(\chi_1,\chi_2)$ as its covariance function which is bounded, symmetric and positive definite with the following spectral decomposition

$$C_{\text{cov}}(\chi_1,\chi_2) = \sum_{n=0}^{\infty} \lambda_n \varphi_n(\chi_1) \varphi_n(\chi_2) \tag{1}$$

where λ_n and $\varphi_n(\chi)$ are the eigenvalues and eigenvectors of the covariance kernel, respectively. The eigenvectors are orthogonal, and can be normalized according to

$$\int_V \varphi_q(\chi) \varphi_n(\chi) d\chi = \delta_{qn} \tag{2}$$

where δ_{qn} is the Kronecker delta function. The eigenpairs $(\lambda_n, \varphi_n(\chi))$ can be obtained through solving the homogeneous Fredholm integral equation

$$\int_V C_{\text{cov}}(\chi_1,\chi_2) \varphi_n(\chi_2) d\chi_2 = \lambda_n \varphi_n(\chi_1) \tag{3}$$

The random process can then be written as

$$H(\chi,\theta) = \bar{H}(\chi) + \underbrace{\sum_{n=1}^{\infty} \sqrt{\lambda_n} \varphi_n(\chi) \xi_n(\theta)}_{H_\sigma(\chi,\theta)} \tag{4}$$

where $\xi_n(\theta)$ is a set of uncorrelated random variables with a zero mean and a unit variance. Moreover, an explicit expression for $\xi_n(\theta)$ can be deduced by multiplying $H_\sigma(\chi,\theta)$ by $\varphi_n(\chi)$ and integrating through the domain V

$$\xi_n(\theta) = \frac{1}{\sqrt{\lambda_n}} \int_V H_\sigma(\chi,\theta) \varphi_n(\chi) d\chi \tag{5}$$

In practice, the random field $H(\chi,\theta)$ is approximated by $\tilde{H}(\chi,\theta)$ after truncating the expansion at the M-th term, i.e.,

$$H(\chi,\theta) = \tilde{H}(\chi,\theta) = \bar{H}(\chi) + \sum_{n=1}^{M} \sqrt{\lambda_n} \varphi_n(\chi) \xi_n(\theta) \tag{6}$$

2.2 PC expansion

PC expansion is built upon the theory of the homogeneous chaos [17], which is defined as elements of the space spanned by Hermite polynomials of Gaussian random variables. For general non-Gaussian random inputs, the optimal exponential convergence rate will not be realized. Xiu and Karniadakis [18] introduced the Wiener–Askey polynomial chaos expansion to the representation of random processes with different probability distributions. The utilization of different type orthogonal polynomials from the Askey scheme also provides a more efficient way to represent general non-Gaussian processes compared with the original Wiener–Hermite expansions. PC expansion is an efficient non-sampling-based method for representing the stochastic processes/fields as an orthogonal polynomial series expansion of a sequence of random variables with deterministic coefficients [18]. A general random process $\alpha(\theta)$, considered as a function of the random variable θ, can be represented in the following form

$$
\begin{aligned}
\alpha(\theta) = a_0\psi_0 &+ \sum_{j1=1}^{\infty} a_{j1}\psi_1\left(\xi_{j1}(\theta)\right) \\
&+ \sum_{j1=1}^{\infty}\sum_{j2=1}^{i_1} a_{j1,j2}\psi_2\left(\xi_{j1}(\theta),\xi_{j2}(\theta)\right) \\
&+ \sum_{j1=1}^{\infty}\sum_{j2=1}^{j1}\sum_{j3=1}^{j2} a_{j1,j2,j3}\psi_3\left(\xi_{j1}(\theta),\xi_{j2}(\theta),\xi_{j3}(\theta)\right)+...
\end{aligned}
\tag{7}
$$

where ψ_p are the terms of order p in the PC expansion, and $a_{j1,j2,j3}$ are deterministic coefficients.

For instance, when the expansion in Eq. (7) is truncated for the two-dimensional case, the PC approximation can be expressed as

$$
\begin{aligned}
\alpha(\theta) = a_0\psi_0 &+ a_1\psi_1(\xi_1) + a_2\psi_1(\xi_2) \\
&+ a_{11}\psi_2(\xi_1,\xi_1) + a_{21}\psi_2(\xi_1,\xi_2) + a_{22}\psi_2(\xi_2,\xi_2) \\
&+ a_{111}\psi_3(\xi_1,\xi_1,\xi_1) + a_{211}\psi_3(\xi_2,\xi_1,\xi_1) + a_{221}\psi_3(\xi_2,\xi_2,\xi_1) + a_{222}\psi_3(\xi_2,\xi_2,\xi_2) + ...
\end{aligned}
\tag{8}
$$

For notational convenience, a one-to-one correspondence can be established between the polynomials $\psi_k(\ )$ and new polynomial functions $\Psi_k(\ )$, such that Eq. (8) can be rewritten as a more compact expression

$$\alpha(\theta) = \sum_{k=0}^{\infty} \hat{a}_k \Psi_k(\xi(\theta)) \tag{9}$$

where $\hat{a}_k$ are the deterministic PC coefficients. The two-dimensional expansion as shown in Eq. (8), in this case, can be expressed as,

$$
\begin{aligned}
\alpha(\theta) = {} & \hat{a}_0 \Psi_0 + \hat{a}_1 \Psi_1(\xi_1) + \hat{a}_2 \Psi_1(\xi_2) \\
& + \hat{a}_{11} \Psi_2(\xi_1) + \hat{a}_{21} \Psi_1(\xi_2) \Psi_1(\xi_1) + \hat{a}_{22} \Psi_2(\xi_2) \\
& + \hat{a}_{111} \Psi_3(\xi_1) + \hat{a}_{211} \Psi_1(\xi_2) \Psi_2(\xi_1) + \hat{a}_{221} \Psi_2(\xi_2) \Psi_1(\xi_1) + \hat{a}_{222} \Psi_3(\xi_2) + \dots
\end{aligned}
\tag{10}
$$

It is worth to note that the polynomials $\Psi_k(\xi(\theta))$ are orthogonal satisfying the relationship

$$\langle \Psi_k \xi(\theta), \Psi_l \xi(\theta) \rangle = \Psi_k^2 \xi(\theta) \delta_{kl} \tag{11}$$

where δ_{kl} is the Kronecker delta. The symbol $\langle \bullet \rangle$ denotes the inner product, and the value of Ψ_k^2 can be calculated analytically [7].

3 Stochastic dynamic system with uncertainties

3.1 Equation of motion of an offshore riser under sea wave loads

The deterministic equation of motion of an offshore riser as shown in Figure 1 subjected to the sea wave loads can be written as

$$m\ddot{x}(t) + c\dot{x}(t) + kx(t) = f(t) \tag{12}$$

where m, c and k are the mass, damping and stiffness matrices of the structure, respectively; x, $\dot{x}$ and $\ddot{x}$ are the displacement, velocity and acceleration response vectors, respectively. $f(t)$ is the sea wave load on the riser. The global mass and stiffness matrices can be obtained by assembling the elemental matrices as

$$m = \sum_{i=1}^{ne} m_i^e \tag{13}$$

$$k = \sum_{i=1}^{ne} k_i^e \tag{14}$$

where $\boldsymbol{m}_i^e = \int \boldsymbol{N}^T (\rho A) \boldsymbol{N} dl$ and $\boldsymbol{k}_i^e = \int \boldsymbol{B}^T (EI) \boldsymbol{B} dl$ are respectively the mass and stiffness matrices of the i-th element, and ne is the number of the elements. $\boldsymbol{N}$ and $\boldsymbol{B}$ are the shape function and strain-displacement matrix for each element; ρ, A, E, I, and l are the mass density, cross-sectional area, Elastic modulus, moment of inertia and the length of each element, respectively. In this study, only the vibration of the risers along the direction of the applied loading is considered. Therefore the distributed drag force along the longitudinal direction can be expressed as [19]

$$f(z,t) = \frac{1}{2} \rho_{water} C_D(z,t) U_{current}(z,t)^2 D + A_D \cos(4\pi f_v + \beta) \tag{15}$$

where z and $C_D(z,t)$ are the distance to the seabed and the time and spatially varying drag coefficient, respectively, f_v, ρ_{water} and β are the non-dimensional vortex shedding frequency, the sea water density and the phase angle respectively; A_D and $U_{current}(z,t)$ are the amplitude of the oscillatory part of the drag force and a function which relates the depth to the ocean surface current velocity.

3.2 Representation of the system parameters

KL expansion can be used to represent the uncertain system parameters. In this study, the uncertain mass density and elastic modulus of the system are considered as independent Gaussian random fields. Taking the mass density as an example, the mass density $\rho(\chi,\theta)$ of the structure is assumed to satisfy Gaussian distribution with the mean value $\bar{\rho}$ and a standard deviation σ_ρ. KL expansion is employed to represent the uncertain mass density as

$$\rho(\chi,\theta) = \bar{\rho} + \tilde{\rho} = \bar{\rho} + \sum_{i1=1}^{K_\rho} \xi_{i1}(\theta) \sqrt{\lambda_{i1}} \varphi_{i1}(\chi) \tag{16}$$

where $\tilde{\rho}$ denotes the random component.

Substituting Eq. (16) into Eq. (13), the stochastic mass matrix of the system can be expressed as two parts:

$$M(\theta) = \bar{M} + \tilde{M} \tag{17}$$

where

8

$$\bar{M} = \sum_{i=1}^{ne} \bar{M}_i^e = \sum_{i=1}^{ne} \left(\int N^T \left(\bar{\rho} A \right) N dl \right) \tag{18}$$

$$\tilde{M} = \sum_{i=1}^{ne} \tilde{M}_i^e = \sum_{i=1}^{ne} \left(\int N^T \left(\sum_{i1=1}^{K_\rho} \xi_{i1} (\theta) \sqrt{\lambda_{i1}} \varphi_{i1} (\chi) A \right) N dl \right) \tag{19}$$

Let $M_{i1}^e = \int N^T \left(\sqrt{\lambda_{i1}} \varphi_{i1} (\chi) A \right) N dl$ and $M_{i1} = \sum_{i1=1}^{ne} M_{i1}^e$, Eq. (19) can be written as

$$\tilde{M} = \sum_{i1=1}^{K_\rho} \xi_{i1} (\theta) M_{i1} \tag{20}$$

Defining $M_{i1=0} = \bar{M}$ and $\xi_{i1=0} (\theta) = 1$, the stochastic mass matrix can be expressed as

$$M(\theta) = \sum_{i1=0}^{K_\rho} \xi_{i1} (\theta) M_{i1} \tag{21}$$

Similarly, the stiffness matrix can be obtained as

$$K(\theta) = \sum_{i2=0}^{K_E} \xi_{i2} (\theta) K_{i2} \tag{22}$$

Substituting Eqs. (21) and (22) into Eq. (12), the equation of motion of the stochastic system can be obtained as

$$M(\theta) \ddot{x}(t) + C \dot{x}(t) + K(\theta) x(t) = f(t) \tag{23}$$

where C is the damping matrix. When the uncertainty in the damping matrix is considered, the damping matrix can be expressed as

$$C = \alpha M(\theta) + \beta K(\theta) = \alpha \left(\sum_{i1=0}^{K_\rho} \xi_{i1} (\omega) M_{i2} \right) + \beta \left(\sum_{i2=0}^{K_E} \xi_{i2} (\omega) K_{i2} \right) \tag{24}$$

3.3 Representation of responses

The output stochastic displacement, velocity and acceleration responses may not follow the Gaussian distributions [20]. A random dimension, denoted as the parameter θ, is introduced in addition to the spatial–temporal dimension. The response vectors of the system can be represented as

$$x(t,\theta) = \left[x_1(t,\theta), x_2(t,\theta), \cdots, x_{dof}(t,\theta) \right]^T \tag{25}$$

$$\dot{\boldsymbol{x}}(t,\theta) = \left[\dot{x}_1(t,\theta), \dot{x}_2(t,\theta), \cdots, \dot{x}_{dof}(t,\theta)\right]^T \tag{26}$$

$$\ddot{\boldsymbol{x}}(t,\theta) = \left[\ddot{x}_1(t,\theta), \ddot{x}_2(t,\theta), \cdots, \ddot{x}_{dof}(t,\theta)\right]^T \tag{27}$$

in which the subscript represents the DOF number of the physical structure.

Since the covariance matrix of nodal acceleration $\ddot{\boldsymbol{x}}(t,\theta)$, velocity $\dot{\boldsymbol{x}}(t,\theta)$ and displacement $\boldsymbol{x}(t,\theta)$ are not known a priori, the output responses can be expanded by using PC expansion according to Eq. (9) with truncations [18]

$$\boldsymbol{x}(t,\theta) = \sum_{j=0}^{m} \boldsymbol{\Psi}_j(\theta)\boldsymbol{U}^j(t) \tag{28}$$

$$\dot{\boldsymbol{x}}(t,\theta) = \sum_{j=0}^{m} \boldsymbol{\Psi}_j(\theta)\dot{\boldsymbol{U}}^j(t) \tag{29}$$

$$\ddot{\boldsymbol{x}}(t,\theta) = \sum_{j=0}^{m} \boldsymbol{\Psi}_j(\theta)\ddot{\boldsymbol{U}}^j(t) \tag{30}$$

where $\boldsymbol{U}^j(t)$ is the vector of the coefficients in the PC expansion of $\boldsymbol{x}(t,\theta)$; $\dot{\boldsymbol{U}}^j(t)$ and $\ddot{\boldsymbol{U}}^j(t)$ are the first and second derivatives of the coefficient vector $\boldsymbol{U}^j(t)$, respectively. m is the dimension of PC expansion, which can be calculated as [21]

$$m + 1 = \frac{(K_\rho + K_E + p)!}{(K_\rho + K_E)!\, p!} \tag{31}$$

where p is the order of the PC expansion.

Substituting Eqs. (21), (22) and (28-30) into Eq. (23) without considering the uncertainty in the damping matrix, we have

$$\left(\sum_{i1=0}^{K_\rho} \xi_{i1}(\theta)\boldsymbol{M}_{i1}\right)\left(\sum_{j=0}^{m} \boldsymbol{\Psi}_j(\theta)\ddot{\boldsymbol{U}}^j(t)\right) + \boldsymbol{C}\left(\sum_{j=0}^{m} \boldsymbol{\Psi}_j(\theta)\dot{\boldsymbol{U}}^j(t)\right)$$
$$+ \left(\sum_{i2=0}^{K_E} \xi_{i2}(\theta)\boldsymbol{K}_{i2}\right)\left(\sum_{j=0}^{m} \boldsymbol{\Psi}_j(\theta)\boldsymbol{U}^j(t)\right) = \boldsymbol{F}(t) \tag{32}$$

Taking the inner product on both sides of the equation with $\boldsymbol{\Psi}_k(\theta)$ and employing the orthogonal property in Eq. (11), we have

$$\sum_{j=0}^{m}\sum_{i1=0}^{K_{\rho}}\left\langle\xi_{i1}(\theta)\varPsi_{j}(\theta),\varPsi_{k}(\theta)\right\rangle M_{i1}\ddot{U}^{j}(t)+\sum_{j=0}^{m}\left\langle\varPsi_{j}(\theta),\varPsi_{k}(\theta)\right\rangle C\dot{U}^{j}(t)$$

$$+\sum_{j=0}^{m}\sum_{i2=0}^{K_{E}}\left\langle\xi_{i2}(\theta)\varPsi_{j}(\theta),\varPsi_{k}(\theta)\right\rangle K_{i2}U^{j}(t)=\left\langle\varPsi_{k}(\theta),F_{f}\right\rangle \qquad (k=0,1,2\cdots m)(33)$$

Rewriting Eq. (33) in the matrix multiplication form, we have

$$
\begin{bmatrix}
M_s^{(0,0)} & M_s^{(0,1)} & \cdots & M_s^{(0,m)} \\
M_s^{(1,0)} & M_s^{(1,1)} & \cdots & M_s^{(1,m)} \\
\vdots & \vdots & \ddots & \vdots \\
M_s^{(m,0)} & M_s^{(m,1)} & \cdots & M_s^{(m,m)}
\end{bmatrix}
\begin{bmatrix}
\ddot{U}^0(t) \\
\ddot{U}^1(t) \\
\vdots \\
\ddot{U}^m(t)
\end{bmatrix}
+
\begin{bmatrix}
C_s^{(0,0)} & C_s^{(0,1)} & \cdots & C_s^{(0,m)} \\
C_s^{(1,0)} & C_s^{(1,1)} & \cdots & C_s^{(1,m)} \\
\vdots & \vdots & \ddots & \vdots \\
C_s^{(m,0)} & C_s^{(m,1)} & \cdots & C_s^{(m,m)}
\end{bmatrix}
\begin{bmatrix}
\dot{U}^0(t) \\
\dot{U}^1(t) \\
\vdots \\
\dot{U}^m(t)
\end{bmatrix}
$$

$$
+
\begin{bmatrix}
K_s^{(0,0)} & K_s^{(0,1)} & \cdots & K_s^{(0,m)} \\
K_s^{(1,0)} & K_s^{(1,1)} & \cdots & K_s^{(1,m)} \\
\vdots & \vdots & \ddots & \vdots \\
K_s^{(m,0)} & K_s^{(m,1)} & \cdots & K_s^{(m,m)}
\end{bmatrix}
\begin{bmatrix}
U^0(t) \\
U^1(t) \\
\vdots \\
U^m(t)
\end{bmatrix}
=
\begin{bmatrix}
F^0(t) \\
F^1(t) \\
\vdots \\
F^m(t)
\end{bmatrix}
\tag{34}
$$

where

$$K_s^{(j,k)}=\sum_{i2=0}^{K_E}\left\langle\xi_{i2}(\theta)\varPsi_{j}(\theta),\varPsi_{k}(\theta)\right\rangle K_{i2} \quad (j,k=0,1,2\cdots m) \tag{35}$$

$$M_s^{(j,k)}=\sum_{i1=0}^{K_\rho}\left\langle\xi_{i1}(\theta)\varPsi_{j}(\theta),\varPsi_{k}(\theta)\right\rangle M_{i1} \quad (j,k=0,1,2,\cdots,m) \tag{36}$$

$$C_s^{(j,k)}=\varPsi_k^2(\theta)\delta_{jk}C \qquad (k=0,1,2,\cdots,m) \tag{37}$$

and

$$F^k=\left\langle\varPsi_k(\theta),f(t)\right\rangle=\begin{cases} f(t),k=0 \\ 0,k=1,2,3,\cdots,m \end{cases} \tag{38}$$

When considering the uncertainties in the damping matrix, using the similar procedure and we have

$$C_s^{(j,k)}=\alpha\left(\sum_{i1}^{K_\rho}\left\langle\xi_{i1}(\theta)\varPsi_{j}(\theta),\varPsi_{k}(\theta)\right\rangle M_{i1}\right)+\beta\left(\sum_{i2}^{K_E}\left\langle\xi_{i2}(\theta)\varPsi_{j}(\theta),\varPsi_{k}(\theta)\right\rangle K_{i2}\right) \tag{39}$$

Eq. (34) can then be simplified as

$$M_s\ddot{U}_s(t)+C_s\dot{U}_s(t)+K_sU_s(t)=F_s(t) \tag{40}$$

The coefficients of PC expansion can be calculated by solving Eq. (40). The DOFs of the stochastic system is equal to $dof \times (m+1)$.

3.4 Model reduction

It should be noted when a large number of KL expansion terms and a high order of PC expansion are involved, the dimensions of the stochastic system as shown in Eq. (33) will increase significantly and the response analysis will be extremely computational intensive. Model reduction technique will be applied to reduce the size of system matrices and improve the compuational efficiency. Only the essential DOFs are kept in the comuptation. In the last several decades, various techniques have been developed for model order reduction, such as Guyan's method [22], Improved Reduced System method [23] and IIRS [24]. The convergence of IIRS used for model reduction has been proved by Friswell [25]. Later it has been successfully used for structural condition assessment [26] and calculating the structural responses and sensitivities [27]. It is noted that the selection of master DOFs may affect the accuracy of modal analysis and response analysis. One of the commonly used criterion is to choose those DOFs with the lowest stiffness to mass ratio in the system matrices. Other methods like Shah and Raymund's scheme [28], element-based node selection method [29] are also proposed to better identify the master DOFs.

IIRS model reduction technique is used in this study, and will be described briefly in this section. The essential DOFs of the stochastic system are selected as the master DOFs in the reduced system. The eigenvalue problem of the stochastic system can be expressed as

$$\boldsymbol{K}_s \boldsymbol{\Phi} = \boldsymbol{M}_s \boldsymbol{\Phi} \Lambda \tag{41}$$

where $\boldsymbol{\Phi}$ and Λ are the eigenvector and eigenvalues respectively. To apply the dynamic condensation scheme for model reduction, Eq. (41) can be rewritten in a partitioned form as

$$\begin{bmatrix} \boldsymbol{K}_{aa} & \boldsymbol{K}_{ab} \\ \boldsymbol{K}_{ba} & \boldsymbol{K}_{bb} \end{bmatrix} \begin{bmatrix} \boldsymbol{\Phi}_{aa} \\ \boldsymbol{\Phi}_{ba} \end{bmatrix} = \begin{bmatrix} \boldsymbol{M}_{aa} & \boldsymbol{M}_{ab} \\ \boldsymbol{M}_{ba} & \boldsymbol{M}_{bb} \end{bmatrix} \begin{bmatrix} \boldsymbol{\Phi}_{aa} \\ \boldsymbol{\Phi}_{ba} \end{bmatrix} \Lambda_{aa} \tag{42}$$

where the subscript a indicated the master DOFs which are kept in the reduced system and b represents the slave DOFs to be eliminated.

To eliminate the slave DOFs, the second row of Eq. (42) can be rearranged to obtain

$$\boldsymbol{\Phi}_{ba} = -\boldsymbol{K}_{bb}^{-1}\boldsymbol{K}_{ba}\boldsymbol{\Phi}_{aa} + \boldsymbol{K}_{bb}^{-1}\left(\boldsymbol{M}_{ba}\boldsymbol{\Phi}_{aa} + \boldsymbol{M}_{bb}\boldsymbol{\Phi}_{ba}\right)\Lambda_{aa} \tag{43}$$

A transformation matrix is defined as

$$\boldsymbol{\Phi}_{ba} = \boldsymbol{t}_{tr}\boldsymbol{\Phi}_{aa} \tag{44}$$

with

$$\boldsymbol{t}_{tr} = -\boldsymbol{K}_{bb}^{-1}\boldsymbol{K}_{ba} + \boldsymbol{K}_{bb}^{-1}\left(\boldsymbol{M}_{ba} + \boldsymbol{M}_{bb}\boldsymbol{t}_{tr}\right)\boldsymbol{\Phi}_{aa}\Lambda_{aa}\boldsymbol{\Phi}_{aa}^{-1} \tag{45}$$

The whole eigenvalue vector can be expressed with only master DOFs

$$\begin{bmatrix} \boldsymbol{\Phi}_{aa} \\ \boldsymbol{\Phi}_{ba} \end{bmatrix} = \begin{bmatrix} \boldsymbol{I}_{aa} \\ \boldsymbol{t}_{tr} \end{bmatrix}\boldsymbol{\Phi}_{aa} = \boldsymbol{T}\boldsymbol{\Phi}_{aa} \tag{46}$$

where $\boldsymbol{I}_{aa}$ is an identity matrix of the size $a \times a$. Substituting Eq. (46) into Eq. (42) and premultiplying $\boldsymbol{T}^T$ on the left of this equation, the reduced system matrices is obtained as

$$\boldsymbol{K}_r = \boldsymbol{T}^T\boldsymbol{K}_s\boldsymbol{T} = \boldsymbol{T}^T\begin{bmatrix} \boldsymbol{K}_{aa} & \boldsymbol{K}_{ab} \\ \boldsymbol{K}_{ba} & \boldsymbol{K}_{bb} \end{bmatrix}\boldsymbol{T} \tag{47}$$

$$\boldsymbol{M}_r = \boldsymbol{T}^T\boldsymbol{M}_s\boldsymbol{T} = \boldsymbol{T}^T\begin{bmatrix} \boldsymbol{M}_{aa} & \boldsymbol{M}_{ab} \\ \boldsymbol{M}_{ba} & \boldsymbol{M}_{bb} \end{bmatrix}\boldsymbol{T} \tag{48}$$

By analysing the above-reduced matrices, a reduced eigenvalue problem of the size $a \times a$ is constructed as

$$\boldsymbol{K}_r\boldsymbol{\Phi}_{aa} = \boldsymbol{M}_r\boldsymbol{\Phi}_{aa}\Lambda_{aa} \tag{49}$$

The eigenvalues can be approximated with

$$\boldsymbol{\Phi}_{aa}\Lambda_{aa}\boldsymbol{\Phi}_{aa}^{-1} = \boldsymbol{M}_r^{-1}\boldsymbol{K}_r \tag{50}$$

Substituting Eq. (50) into Eq. (45), the transformation matrix can be obtained as

$$\boldsymbol{t}_{tr} = -\boldsymbol{K}_{bb}^{-1}\boldsymbol{K}_{ba} + \boldsymbol{K}_{bb}^{-1}\left(\boldsymbol{M}_{ba} + \boldsymbol{M}_{bb}\boldsymbol{t}_{tr}\right)\boldsymbol{M}_r^{-1}\boldsymbol{K}_r \tag{51}$$

Since Eq. (51) is nonlinear, the iterative form is given as

$$\boldsymbol{t}_{tr}^{(it)} = -\boldsymbol{K}_{bb}^{-1}\boldsymbol{K}_{ba} + \boldsymbol{K}_{bb}^{-1}\left(\boldsymbol{M}_{ba} + \boldsymbol{M}_{bb}\boldsymbol{t}_{tr}^{(it-1)}\right)\left(\boldsymbol{M}_r^{(it-1)}\right)^{-1}\boldsymbol{K}_r^{(it-1)} \tag{52}$$

The iterative form of the reduced matrices can be constructed as

$$M_r^{(it-1)} = \left(T^{(it-1)}\right)^T M_s T^{(it-1)} = \left(T^{(it-1)}\right)^T \begin{bmatrix} M_{aa} & M_{ab} \\ M_{ba} & M_{bb} \end{bmatrix} T^{(it-1)} \tag{53}$$

$$K_r^{(it-1)} = \left(T^{(it-1)}\right)^T K_s T^{(it-1)} = \left(T^{(it-1)}\right)^T \begin{bmatrix} K_{aa} & K_{ab} \\ K_{ba} & K_{bb} \end{bmatrix} T^{(it-1)} \tag{54}$$

The eigenvalues and the associated eigenvectors of the reduced stochastic system after (*it*-1)th iteration are estimated by solving the generalized eigenproblem as

$$K_r^{(it)} \boldsymbol{\Phi}_{aa}^{(it)} = K_r^{(it)} \boldsymbol{\Phi}_{aa}^{(it)} \Lambda_{aa}^{(it)} \tag{55}$$

Eq. (53) and (54) will continue until the convergence criteria is satisfied, which is defined as

$$\frac{\left\| \Lambda_{aa}^{(it)} - \Lambda_{aa}^{(it-1)} \right\|}{\left\| \Lambda_{aa}^{(it)} \right\|} \leq Tol \tag{56}$$

The details of IIRS method can be found in [24, 25, 30].

The Rayleigh damping model is defined for the reduced stochastic system

$$C_r = \alpha M_r + \beta K_r \tag{57}$$

The reduced matrices, i.e., M_r, K_r and C_r, will be used for the stochastic dynamic response analysis by using Eq. (40). The associated reduced coefficients of PC expansions, $\ddot{U}_r(t)$, $\dot{U}_r(t)$ and $U_r(t)$ are obtained by using the mode superposition method [31]. After obtaining the coefficients of PC expansions, the mean value of nodal displacements $MEAN_U$ can be evaluated as

$$MEAN_U = U_r^0(t) \tag{58}$$

The variance of nodal displacements VAR_U is obtained as

$$VAR_U = \sum_{j=1}^{m} \left[U_r^j(t) \right]^2 \Psi_j^2(\theta) \tag{59}$$

4 Numerical Studies

4.1 Beam model

A two-dimensional finite element model is built by using Matlab to simulate a marine riser, as shown in Figure 1. The length of the riser is 100m, and the outer diameter is 0.1524 m. The riser is modeled with 20 Euler beam elements with each having 2 nodes and 4 DOFs. The bottom of the riser is considered as a fixed support. Totally the structure has 40 DOFs. The flexural rigidity (*EI*) and the mass density (mass per unit length) are assumed as two independent Gaussian random variables with mean values of 4.0×10^{10} N/m^2 and 15 kg/m, respectively. Each of them is assumed to have the spatial correlation represented as a Gaussian covariance kernel as follows

$$C_{\text{cov}}(z_1, z_2) = \sigma^2 e^{-\left(|z_1 - z_2|^2 / a^2\right)} \tag{60}$$

where σ is the standard deviation of the system parameter. The parameter a and the expression $|z_1 - z_2|$ denote the correlation length and the distance between two points in a spatial domain of interest, respectively. In this study, 20% uncertainties in the mass density and flexural rigidity are considered, and the correlation length is defined as 30m.

The riser, assumed at rest initially, is excited by the sea wave loads. The ocean surface current velocity $U_{current}(t)$ is modeled as a mean flow with sinusoidal components to simulate the riser with an average deflected profile. The sinusoids are assumed to have frequencies $\omega = \{0.867, 1.827, 2.946, 4.282\}$ Hz. The current $U_{current}(t)$ can be express as

$$U_{current}(t) = \bar{U} + U_m \sum_{i=1}^{4} \sin(\omega_i t) \tag{61}$$

where $\bar{U} = 2m/s$ is the mean flow current and $U_m = 0.2$ is the amplitude of the oscillating flow. The surface current generated by Eq. (61) is shown in Figure 2. The full current load is applied from z=100 to 70 m, and the load is linearly declining from z=70 to the ocean floor z=0, to simulate a depth dependent ocean current profile $U_{current}(z,t)$. The excitation *f(z,t)* is simulated by using Eq. (15) with C_D=1.361, β=0, and f_v=2.625. These parameters to simulate the current loading are selected from an existing study [3].

The uncertainty in damping is also considered in the numerical simulation. The damping matrix is obtained from Eq. (39) in which the damping model coefficients defined as $\alpha = 0.6263$ and

$\beta = 0.0003$, which are calculated based on the mean values of the first two natural frequencies and the assumed damping ratio 2% for all the modes. It should be noted that the responses under the sea wave loads are analysed, that means, the force to the top end of the riser due to the floating platform is not considered.

4.1.1 Calculations without model reduction

Figure 3(a) shows the eigenvectors associated with the defined Gaussian covariance kernel for given values of σ and the correlation length, and Figure 3(b) shows the corresponding eigenvalues. The eigenvectors and eigenvalues are obtained from the discrete KL method [32]. Due to the fast decay of the eigenvalues, the first six terms are used in Eq. (1) to generate the random fields. Figure 3(c) shows different samples of random field realizations generated by the Gaussian covariance kernel. The generation of random fields of flexural rigidity can also be obtained with a similar procedure.

Numerical studies without using model reduction technique are conducted. A convergence study with different numbers of MCS simulation runs is conducted to obtain the statistics, i.e. the mean value and variance of the horizontal deformation at the top of the riser at 50s. The results are shown in Figure 4. It is shown that the statistical result from 50,000 simulations is converged, however, requiring the computational time of 16 hours with a computer of an i7-6770 CPU and 32 GB RAM. These response statistics will be taken as the reference values for comparison.

Studies by using different orders of PC expansion for stochastic dynamic responses are conducted to investigate the effect of the order of PC expansion on the accuracy of the stochastic response analysis. Figures 5 and 6 show the comparisons of the mean responses and variances at the top and middle span of the riser from MCS and SFEM with different orders of PC expansions. The results with different PC expansion orders indicate that a higher order of PC expansion will achieve a better accuracy, particularly for the variance. The computational time with different PC expansion orders can be found in Table 1. The numbers of DOFs of the stochastic system in Eq. (33) are 420, 3640 and 18200 repsectively when the order of PC expansion equals to 1, 2, and 3, respectively. The computational time for each case are 11s, 109s and 2519s, respectively. Although a better accuracy can be accomplished with a higher PC order in SFEM, the computational load also increases significantly.

This is the reason why the model reduction technique is considered to maintain the similar acceptable accuracy level but reduce the intensive computation requirement. Figures 7 and 8 show the convergence of the probability density function (PDF) and cumulative distribution function (CDF) of the responses at the top and middle span of the riser at 50s with different orders of PC expansion. It is also proven that a higher order in PC expansion would improve the accuracy in obtaining the PDF and CDF of calculated stochastic responses.

4.1.2 Calculations with model reduction

In this section, the rotational DOFs are defined as the slave and unfavorable DOFs since they are not of signficant interest and usually the responses at the translational DOFs are used in structural response analysis and design. The corresponding terms in the PC expansions associated with those slave DOFs are eliminated by using the described IIRS technique in Section 3.4. The calculation results from SFEM in the above Section 4.1.1 are selected as reference values for comparison when a different number of vibration modes are included in the model reduction to calculate the dynamic responses.

It has been demonstrated that a good accuracy is achieved with the order of PC expansions equal to 3. The computational results with the order of PC expansion equal to 3 are presented in this section. Figure 9 shows the convergence of the obtained results with different numbers of included modes. The coefficients of the PC expansion match well with the true values when the first 30% modes (2730 modes in this study) are involved, indicating that the error caused by the model reduction is minimal. The displacement variance at the top of the riser when the first 30% modes are included in the model reduction is shown in Figure 10, comparing with the result obtained without model reduction. These results demonstrate that the same accuracy can be achieved when the model reduction is used in the stochastic dynamic response analysis. However, the computational workload is reduced with a smaller system matrix size. It is noted that in this case, the computational time with using model reduction is decreased from 2519s to 1436s.

4.2 Hollow cylinder model

To investigate whether this proposed approach is applicable for stochastic response analysis of a relatively large scale structure, a three-dimensional finite element model of a riser is further built with shell elements for numerical investigations in this section. The length of the riser is 4m, and the outer radius is 0.1m. The thickness is 10mm. The mean values of the mass density and elastic modulus of the riser are 7850 kg/m^3 and 200 GPa, respectively. The mesh size of the finite element model is defined as 0.5m in the longitudinal direction. The cross-section is divided into 16 elements. Each shell element has 4 nodes and each node has 6 DOFs. The finite element model has 144 nodes, 128 elements and 864 DOFs in total, as shown in Figure 11. The riser is fixed at the bottom, and is excited by a distributed non-uniform transverse load in the y-direction, which is modeled as multiple sinusoidal components $f(t) = 10\sin(\pi t) + 2\sin(4\pi t)\ KN$. The full current load is applied from z=4m to 3m and linearly declines to zero from 3m to the ocean floor.

Same as the previous numerical study, the uncertainty in damping is also considered. The damping ratios are assumed as 2% for all the modes, and the damping coefficients can be obtained as $\alpha = 3.5969$ and $\beta = 5.31 \times 10^{-5}$. The random field is described by a three dimensional exponential covariance kernel as

$$C_{\text{cov}}\left((x_1, y_1, z_1),(x_2, y_2, z_2)\right) = \sigma^2 e^{-\left((x_1-x_2)^2/l_x^2 + (y_1-y_2)^2/l_y^2 + (z_1-z_2)^2/l_z^2\right)} \tag{62}$$

with the correlation lengths $l_x = l_y = 0.05$ and $l_z = 1$. Uncertainties in the elastic modulus and mass density are considered separately to understand the structural vibration behavior. 10% uncertainty level is considered for those two parameters.

MCS with 50000 runs are carried out to obtain the reference values of the response statistics for comparison with the SFEM results, taking more than 220 hours because of the complexity of the used model. KL expansions with the first four eigenvalues and eigenvectors are employed to generate the random fields for system parameters. The third order PC expansion is used to approximate the output responses. The vibration along the x direction is very small since the loads are applied in the y-z plane. Therefore, the DOFs along the x direction and all the rotational DOFs are taken as the slave DOFs and eliminated by using IIRS. When using the mode superposition to calculate the dynamic responses, the

first 30% modes (2688 modes in this study) are included. The same computational procedure is followed as the numerical studies in Section 4.1.

The response statistics at a critical point at the top of the riser as shown in Figure 11 are obtained. Figure 12 shows the mean value and variance of the displacement at the critical point when the uncertainty in the elastic modulus is considered. The results from SFEM with and without model reduction are shown in Figure 12, indicating a well agreement with those obtained from MCS. The required computational time with and without model reduction are 2052s and 6144s, respectively. Compared with the intensive computational load required for MCS, the proposed approach with model reduction technique can significantly improve the efficiency of stochastic analysis but has no significant impact on the accuracy. Figure 13 shows the PDF and CDF of the displacement response at the critical point from MCS and SFEM with model reduction at the time instant with the maximum deformation. The results from MCS and SFEM with model reduction are well matched, which demonstrates that the accuracy in obtaining the response statistics when using model reduction is not affected significantly. Figure 14 shows the contour of the displacement variance along the whole riser due to the uncertainty in the mass density at $t=4.8s$. The amplitude of variance reduces from the top to the bottom, maybe because more significant vibrations are observed at the top of the model. The variance due to the uncertainty in elastic modulus is larger than that due to the uncertainty in mass density when comparing the variances as shown in Figures 12 and 14indicating that the uncertainty in the elastic modulus has a more significant effect on the response statistics in the stochastic dynamic analysis of this model.

5 Conclusions

This paper performs the stochastic dyanmic response analysis of offshore risers considering the uncertainty in material properties. The uncertainties in the mass density and elastic modulus are considered. The random inputs are represented by using the KL expansion and random outputs are represented by PC expansion. The coefficients of PC expansion of the slave DOFs are eliminated with a mode reduction technique, such as IIRS. The response statistics are obtained and compared with those from MCS. Two numerical examples are presented in this paper. Results show that a high order

PC expansion is required to represent the random output, and using the model reduction technique has no significant effect on the accuracy in the stochastic response analysis but significantly reduces the computational time. The results from the proposed approach based on SFEM and model reduction match well with those from MCS, while the computational time is much less.

Acknowledgements

References

[1] R.D. Blevins, Flow-induced vibration, 2nd Edition, Van Nostrand Reinhold, 1990.

[2] S. Lei, W.-S. Zhang, J.-H. Lin, Q.-J. Yue, D. Kennedy, F. Williams, Frequency domain response of a parametrically excited riser under random wave forces, Journal of Sound and Vibration, 333 (2014) 485-498.

[3] R.I. Tsukada, C.K. Morooka, A numerical procedure to calculate the VIV response of a catenary riser, Ocean Engineering, 122 (2016) 145-161.

[4] Q. Han, Y. Ma, W. Xu, Y. Lu, A. Cheng, Dynamic characteristics of an inclined flexible cylinder undergoing vortex-induced vibrations, Journal of Sound and Vibration, 394 (2017) 306-320.

[5] F. Rivero-Angeles, A. Vázquez-Hernández, U. Martinez, Vibration analysis for the determination of modal parameters of steel catenary risers based on response-only data, Engineering Structures, 59 (2014) 68-79.

[6] Y. Gao, Z. Zong, L. Sun, Numerical prediction of fatigue damage in steel catenary riser due to vortex-induced vibration, Journal of Hydrodynamics, Ser. B, 23 (2011) 154-163.

[7] R.G. Ghanem, P.D. Spanos, Stochastic finite elements: a spectral approach, Courier Corporation, 2003.

[8] K. Sepahvand, Stochastic finite element method for random harmonic analysis of composite plates with uncertain modal damping parameters, Journal of Sound and Vibration, 400 (2017) 1-12.

[9] S.Q. Wu, S.S. Law, Evaluating the response statistics of an uncertain bridge–vehicle system, Mechanical Systems and Signal Processing, 27 (2012) 576-589.

[10] M. Anders, M. Hori, Stochastic finite element method for elasto‐plastic body, International Journal for Numerical Methods in Engineering, 46 (1999) 1897-1916.

[11] K. Bi, H. Hao, C. Li, H. Li, Stochastic seismic response analysis of buried onshore and offshore pipelines, Soil Dynamics and Earthquake Engineering, 94 (2017) 60-65.

[12] J. Foo, Z. Yosibash, G.E. Karniadakis, Stochastic simulation of riser-sections with uncertain measured pressure loads and/or uncertain material properties, Computer Methods in Applied Mechanics and Engineering, 196 (2007) 4250-4271.

[13] J.W. He, Y.M. Low, Predicting the Probability of Riser Collision Under Stochastic Excitation and Multiple Uncertainties, Journal of Offshore Mechanics and Arctic Engineering, 135 (2013) 031602.

[14] M.E. Mousavi, Z. Reza, S. Upadhye, V. Vijayaraghavan, K. Haverty, A Simplified Method for Quantitative Reliability and Integrity Analysis of Steel Catenary Risers, Journal of Offshore Mechanics and Arctic Engineering, 138 (2016) 011601.

[15] W. Qiu, J.S. Junior, D. Lee, H. Lie, V. Magarovskii, T. Mikami, J.-M. Rousset, S. Sphaier, L. Tao, X. Wang, Uncertainties related to predictions of loads and responses for ocean and offshore structures, Ocean Engineering, 86 (2014) 58-67.

[16] S. Huang, S. Quek, K. Phoon, Convergence study of the truncated Karhunen-Loeve expansion for simulation of stochastic processes, International journal for numerical methods in engineering, 52 (2001) 1029-1043.

[17] N. Wiener, The Homogeneous Chaos, American Journal of Mathematics, 60 (1938) 897-936.

[18] D.B. Xiu, G.E. Karniadakis, The Wiener-Askey polynomial chaos for stochastic differential equations, SIAM Journal on Scientific Computing, 24 (2002) 619-644.

[19] B. How, S. Ge, Y. Choo, Active control of flexible marine risers, Journal of Sound and Vibration, 320 (2009) 758-776.

[20] D. Xiu, G.E. Karniadakis, Modeling uncertainty in flow simulations via generalized polynomial chaos, Journal of Computational Physics, 187 (2003) 137-167.

[21] B. Sudret, A. Der Kiureghian, Stochastic finite element methods and reliability: a state-of-the-art report, Department of Civil and Environmental Engineering, University of California Berkeley, CA, 2000.

[22] R.J. Guyan, Reduction of stiffness and mass matrices, AIAA journal, 3 (1965) 380-380.

[23] J.H. Gordis, An analysis of the improved reduced system (IRS) model reduction procedure, 10th International Modal Analysis Conference, 1992, pp. 471-479.

[24] M. Friswell, S. Garvey, J. Penny, Model reduction using dynamic and iterated IRS techniques, Journal of sound and vibration, 186 (1995) 311-323.

[25] M. Friswell, S. Garvey, J. Penny, The convergence of the iterated IRS method, Journal of Sound and Vibration, 211 (1998) 123-132.

[26] J. Li, S. Law, Damage identification of a target substructure with moving load excitation, Mechanical Systems and Signal Processing, 30 (2012) 78-90.

[27] S. Weng, W. Tian, H. Zhu, Y. Xia, F. Gao, Y. Zhang, J. Li, Dynamic condensation approach to calculation of structural responses and response sensitivities, Mechanical Systems and Signal Processing, 88 (2017) 302-317.

[28] V. Shah, M. Raymund, Analytical selection of masters for the reduced eigenvalue problem, International Journal for Numerical Methods in Engineering, 18 (1982) 89-98.

[29] M. Cho, H. Kim, Element-based node selection method for reduction of eigenvalue problems, AIAA journal, 42 (2004) 1677-1684.

[30] D. Choi, H. Kim, M. Cho, Iterative method for dynamic condensation combined with substructuring scheme, Journal of Sound and Vibration, 317 (2008) 199-218.

[31] G. Borino, G. Muscolino, Mode-superposition methods in dynamic analysis of classically and non‐classically damped linear systems, Earthquake engineering & structural dynamics, 14 (1986) 705-717.

[32] C.A. Schenk, G.I. Schuëller, Uncertainty assessment of large finite element systems, Springer Science & Business Media, 2005.

Table 1 Computational time for MCS and SFEM without model reduction

	Case 1	Case 2	Case 3	MCS
PC order	1	2	3	-
Matrix size ($m \times dof$)	13×40	91×40	455×40	40
Computation time	11s	109s	2519s	16 hours
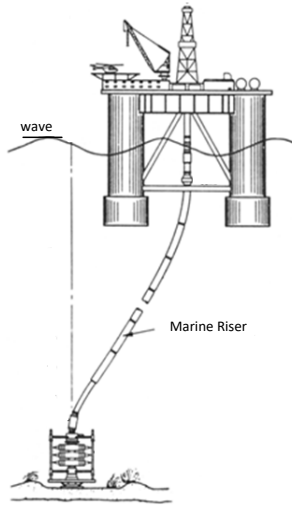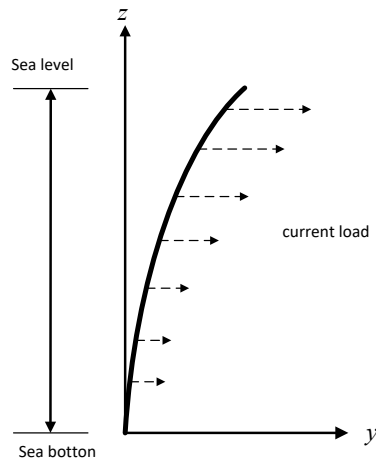
(a) Marine riser   (b) Simplified model   (c) Numerical model
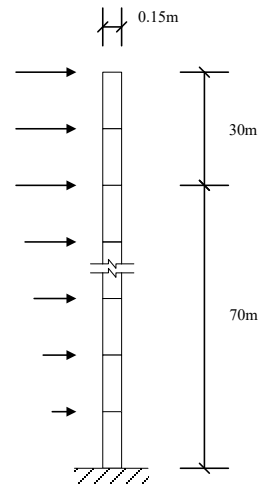
Figure 1 Schematic marine riser, a simplified model and the corresponding numerical model
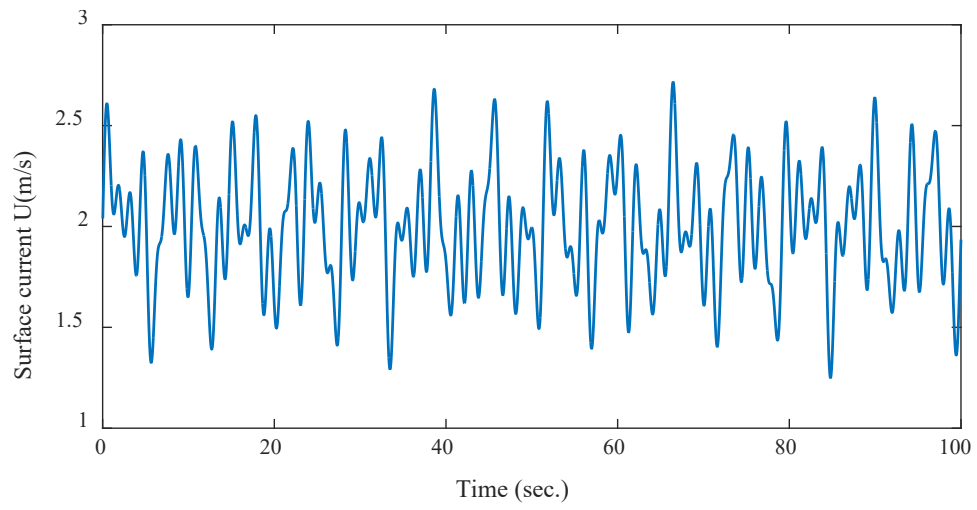
Figure 2 Time history of the applied surface ocean current velocity
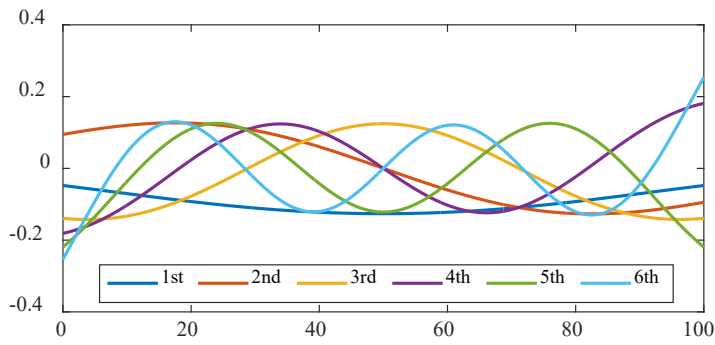
(a) Eigenvectors
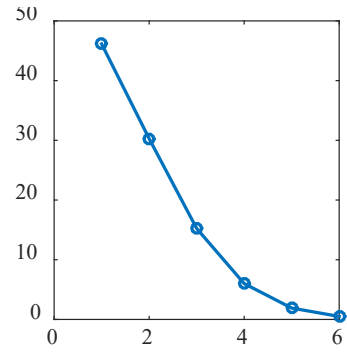
(b) Eigenvalue
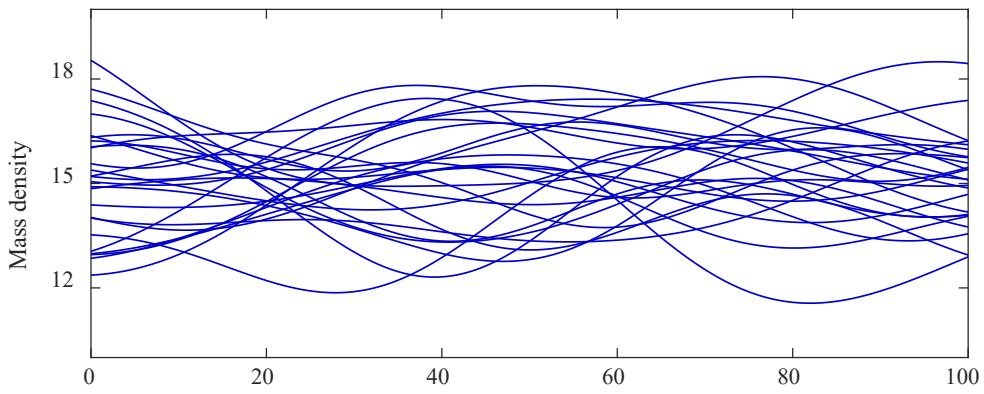
(c) Random field realizations

Figure 3 Generation of random fields by using KL expansion
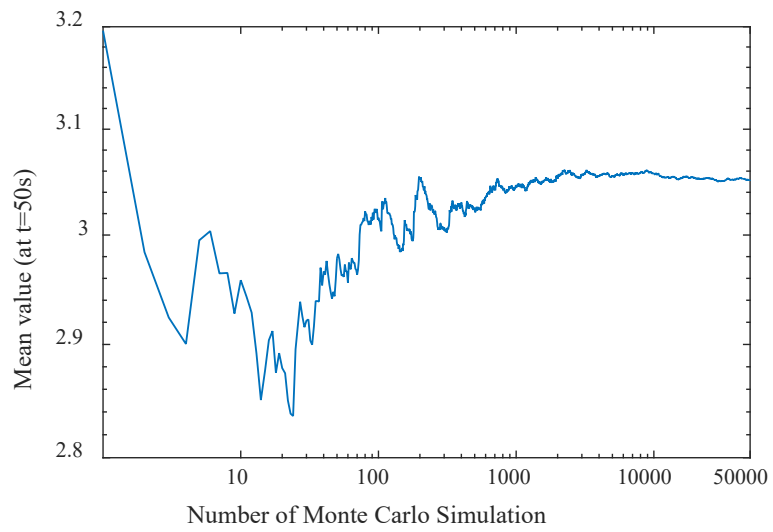
(a) Convergence of mean value with different number of MCS from the top of riser at t=50s
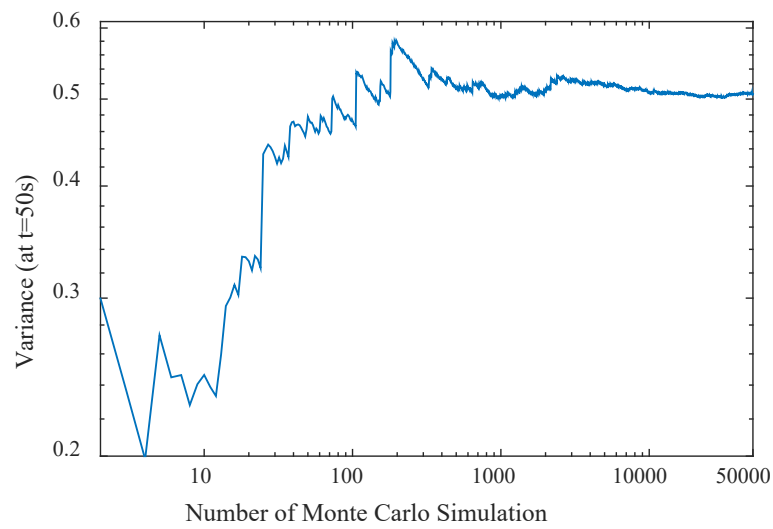
(b) Convergence of variance with different number of MCS from the top of riser at t=50s

Figure 4 Convergence analysis of MCS analysis
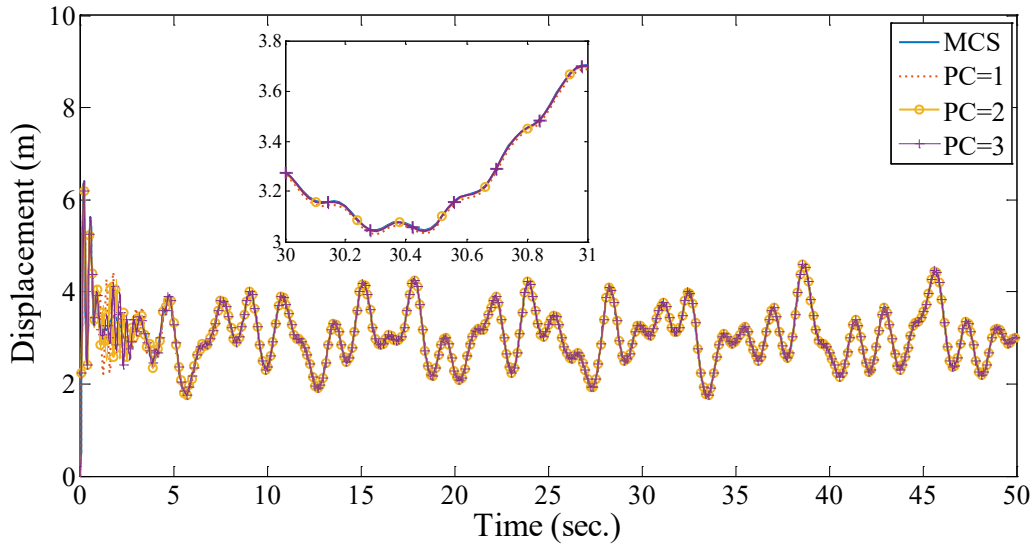
(a) Displacement at the top of riser
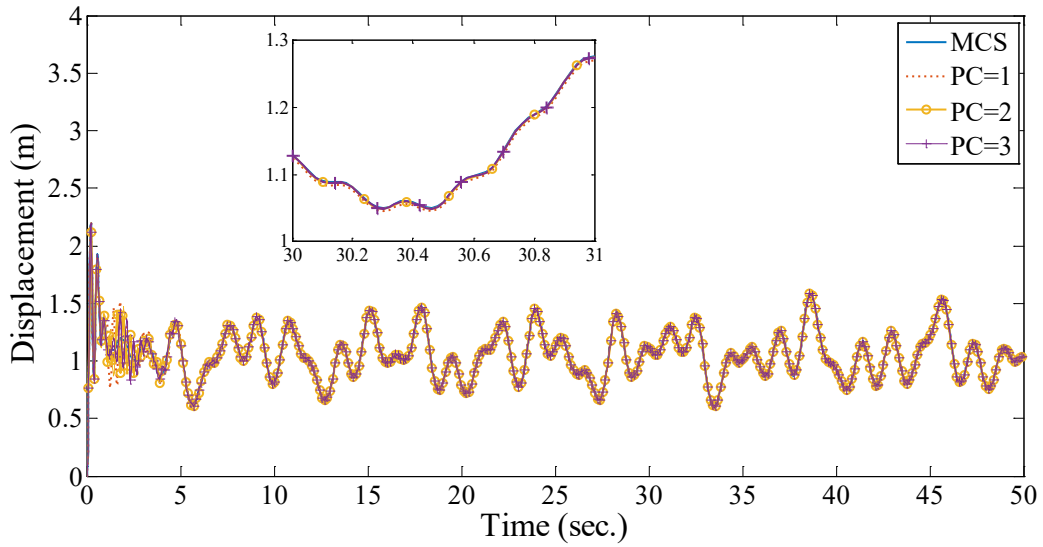
(b) Displacement at the middle span of riser

Figure 5 Mean value of the riser from SFEM and MCS
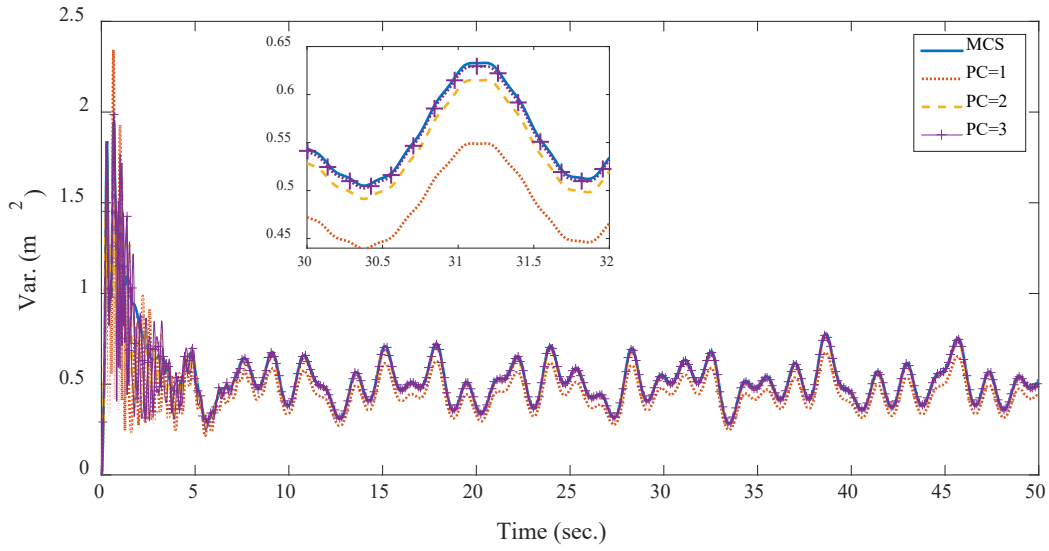
(a) Displacement variance at the top of riser
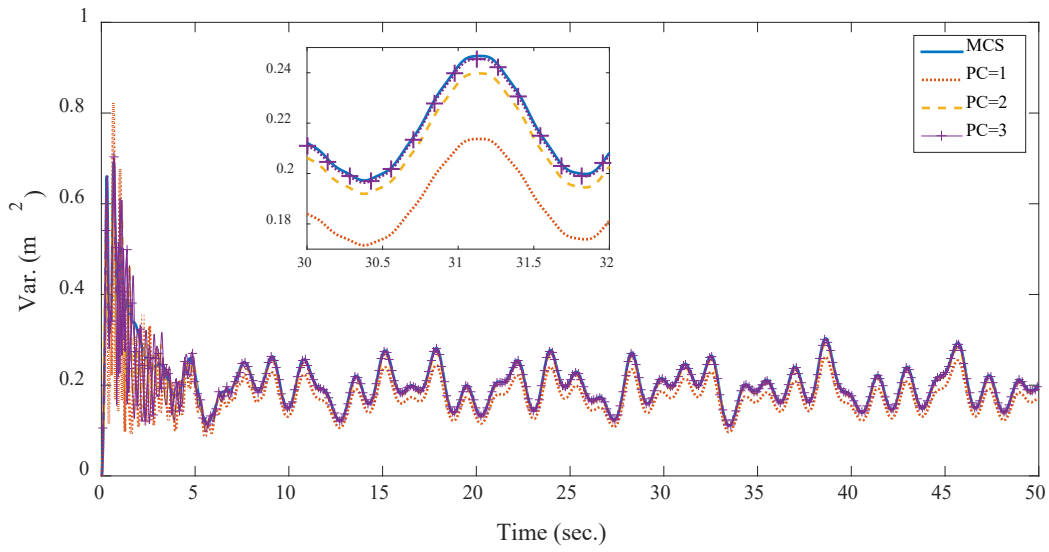
(b) Displacement variance at the middle span of riser

Figure 6 Variance of the riser from SFEM and MCS
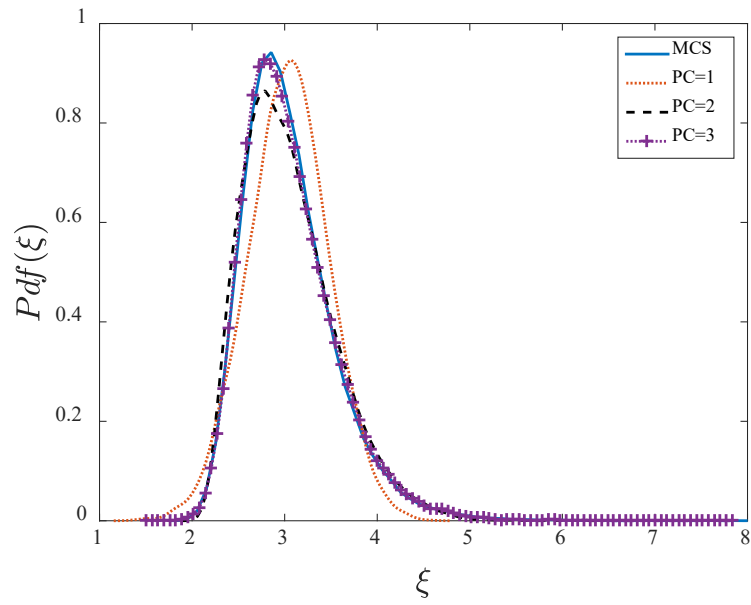
(a) PDF
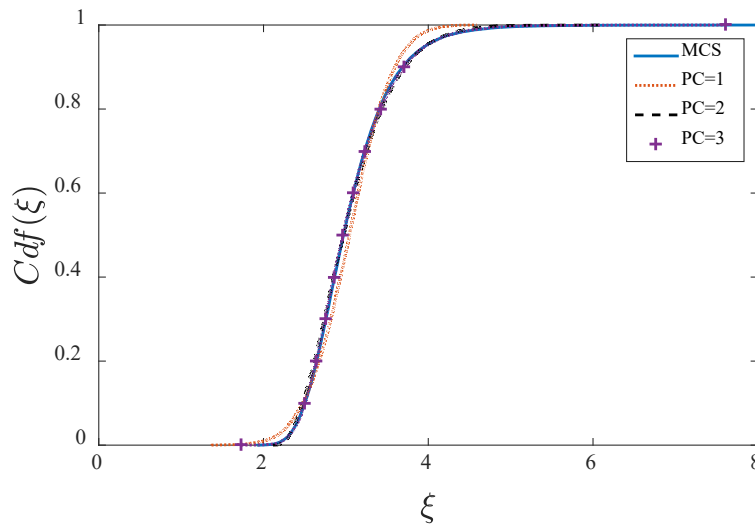
(b) CDF

Figure 7 PDF and CDF of the displacement response at the top of riser (*t*=50s)

from MCS and SFEM with different orders of PC expansion
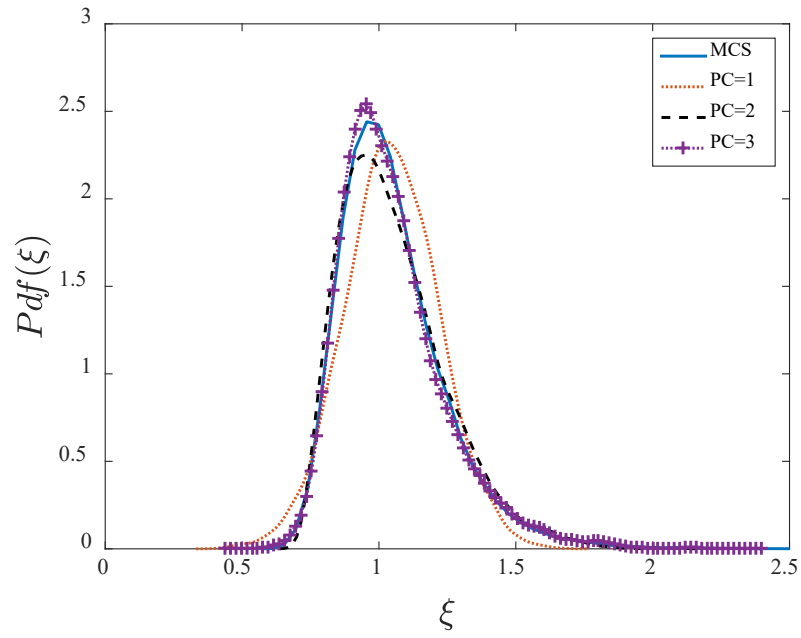
(a) PDF
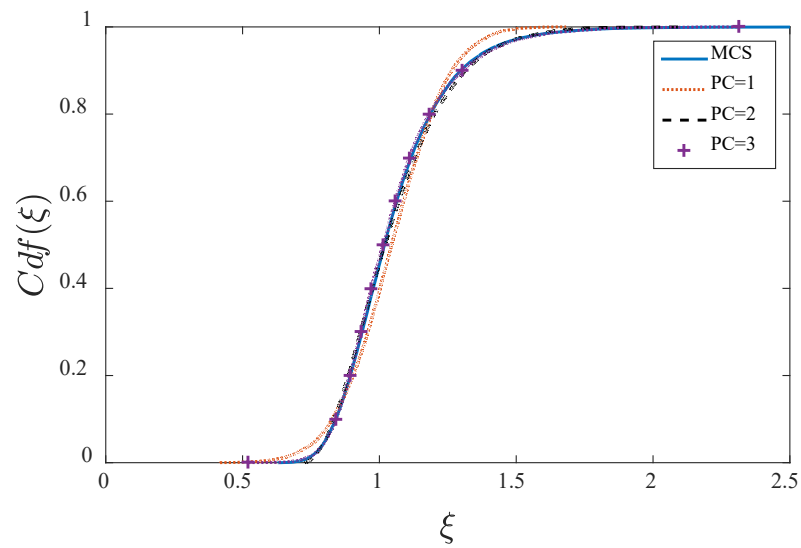
(b) CDF

Figure 8 PDF and CDF of the displacement response at the middle span of the riser (t=50s) from

SFEM and MCS
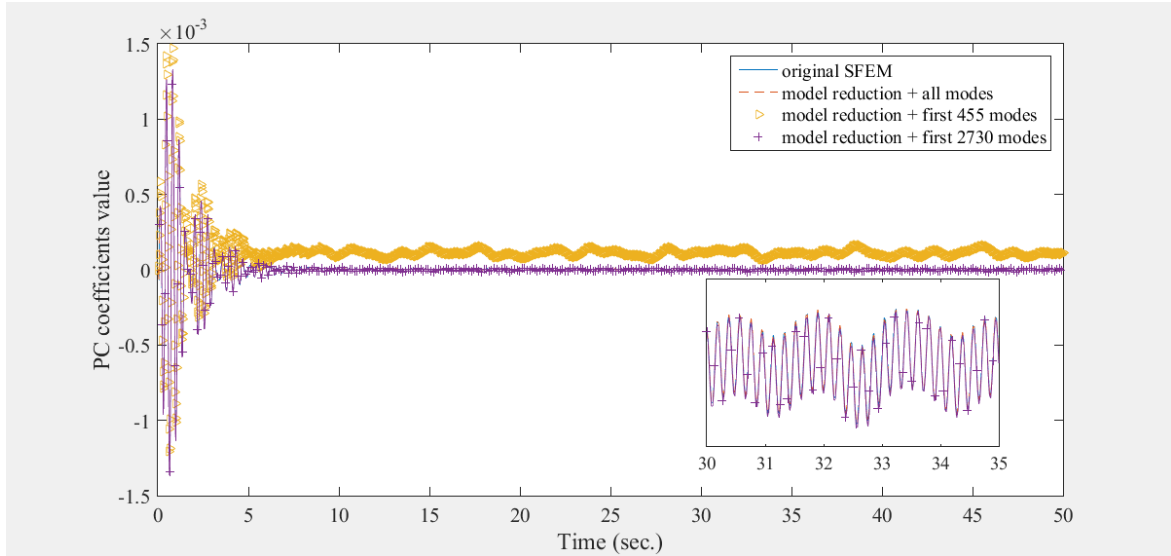
Figure 9 PC coefficients obtained with different number of modes
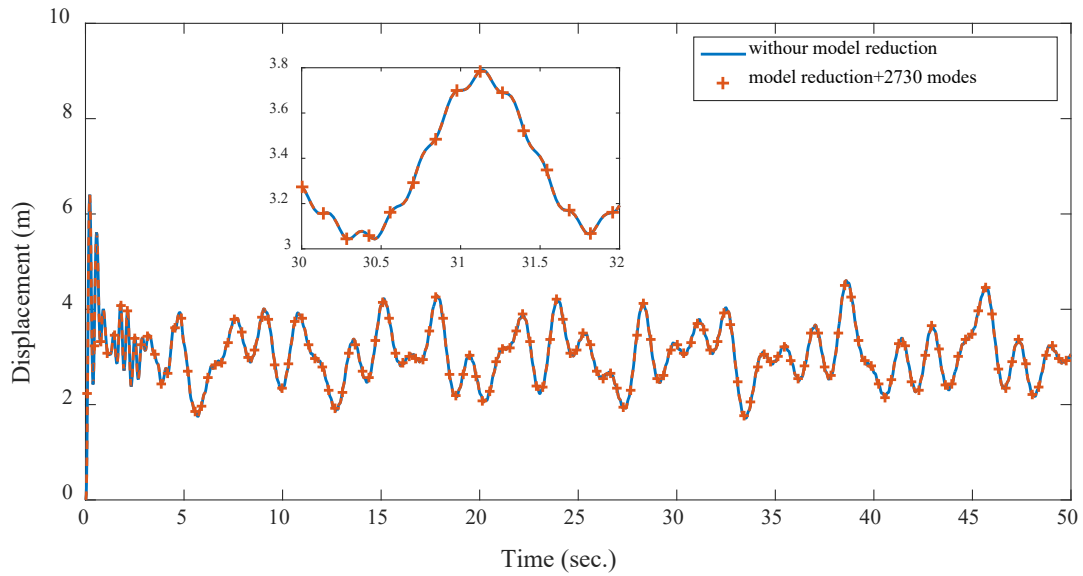
(a) Mean value of displacement at the top from SFEM with/without model reduction when PC=3
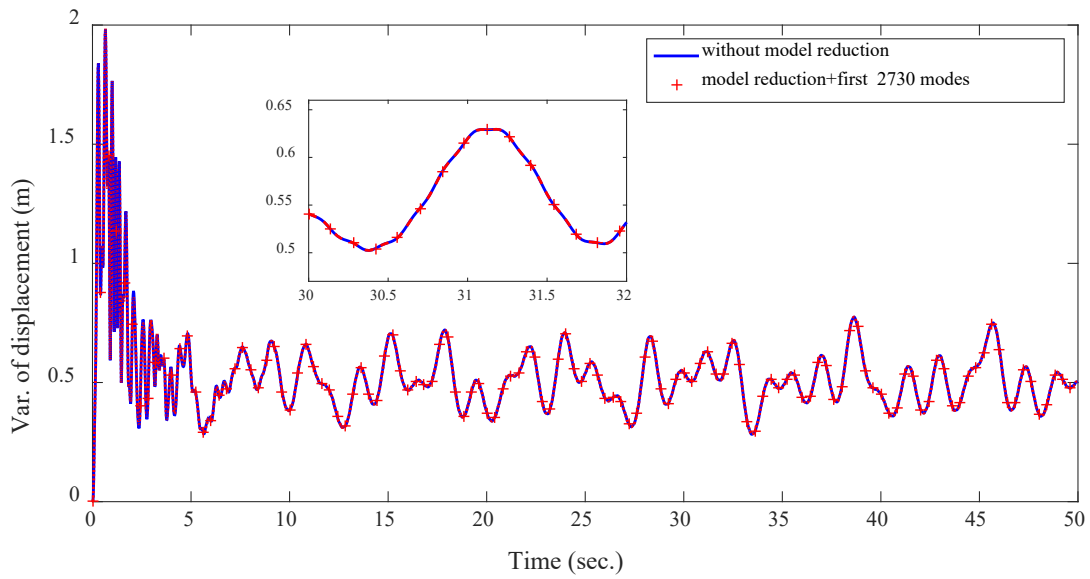
(b) Variance of displacement at the top from SFEM with/without model reduction when PC=3

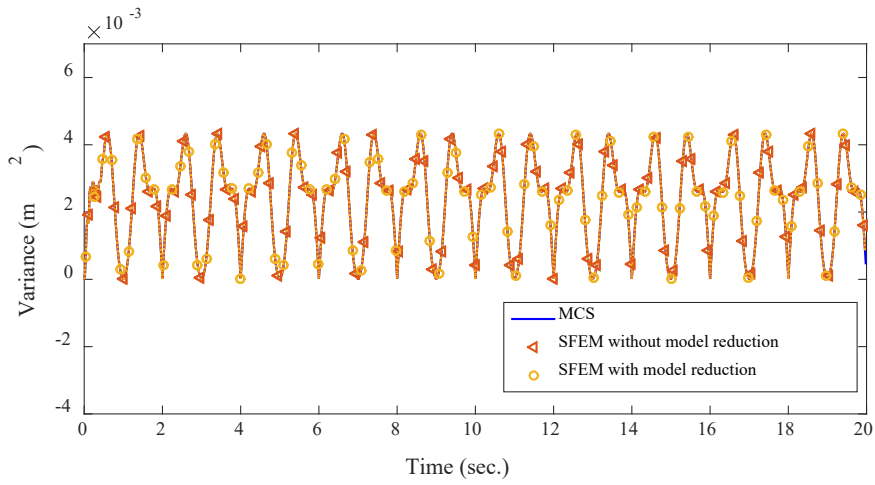Figure 10 Response statistics at the top of riser from SFEM with/without model reduction

Critical point: (0, 0.1, 4)

wave loading
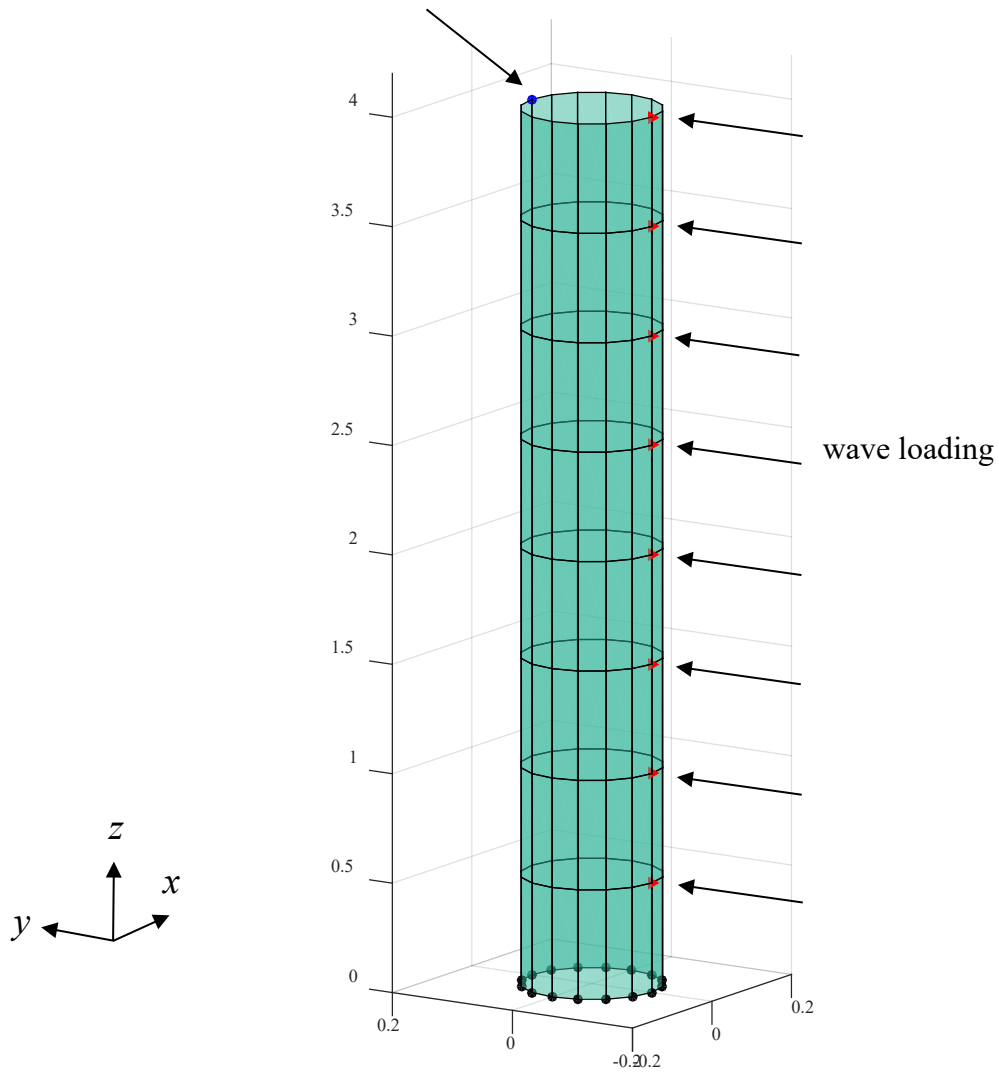
Figure 11 Hollow cylinder model
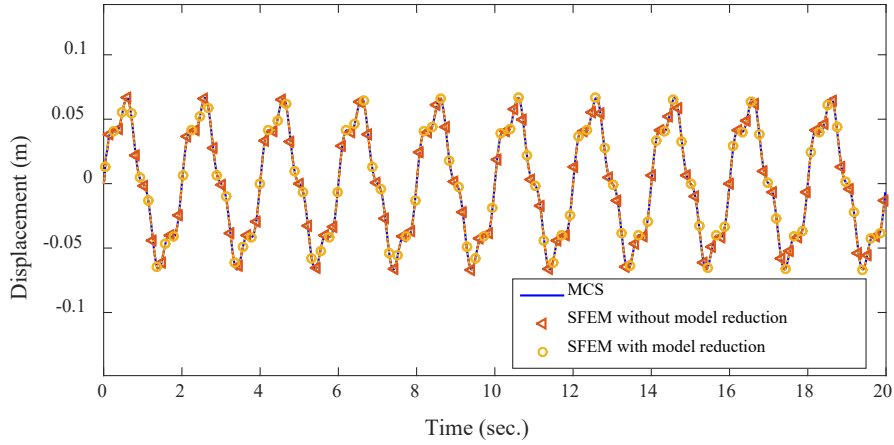
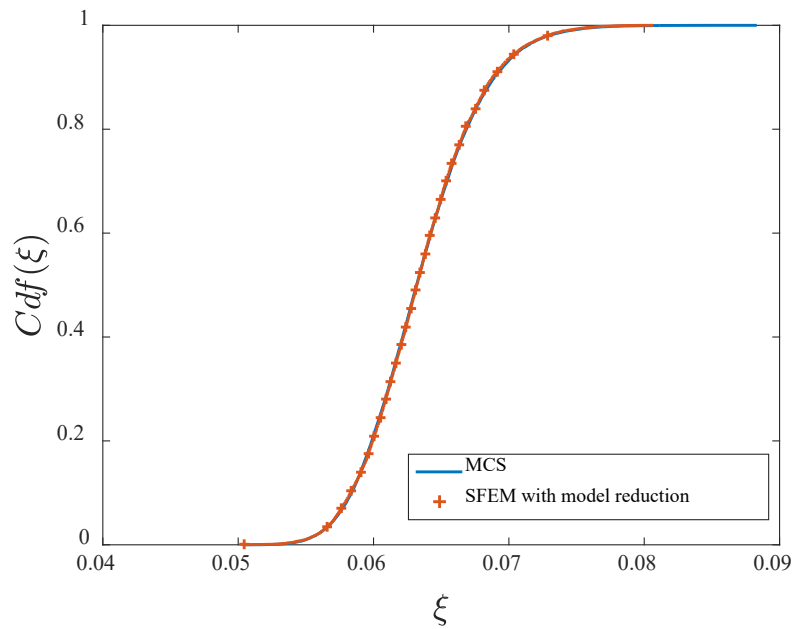(a) Mean value of the displacement at the critical point along the *y*-direction

(b) Variance of the displacement at the critical point along the *y*-direction

Figure 12 Response statistics at the critical point from

SFEM with/without mode reduction
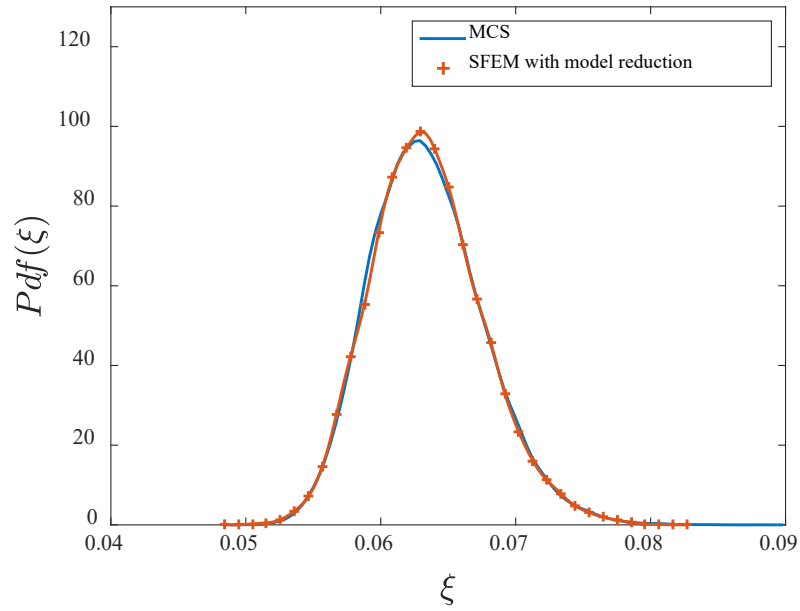
(a) PDF

(b) CDF

Figure 13 PDF and CDF of the displacement response along the y-direction at the critical point from MCS and SFEM with model reduction
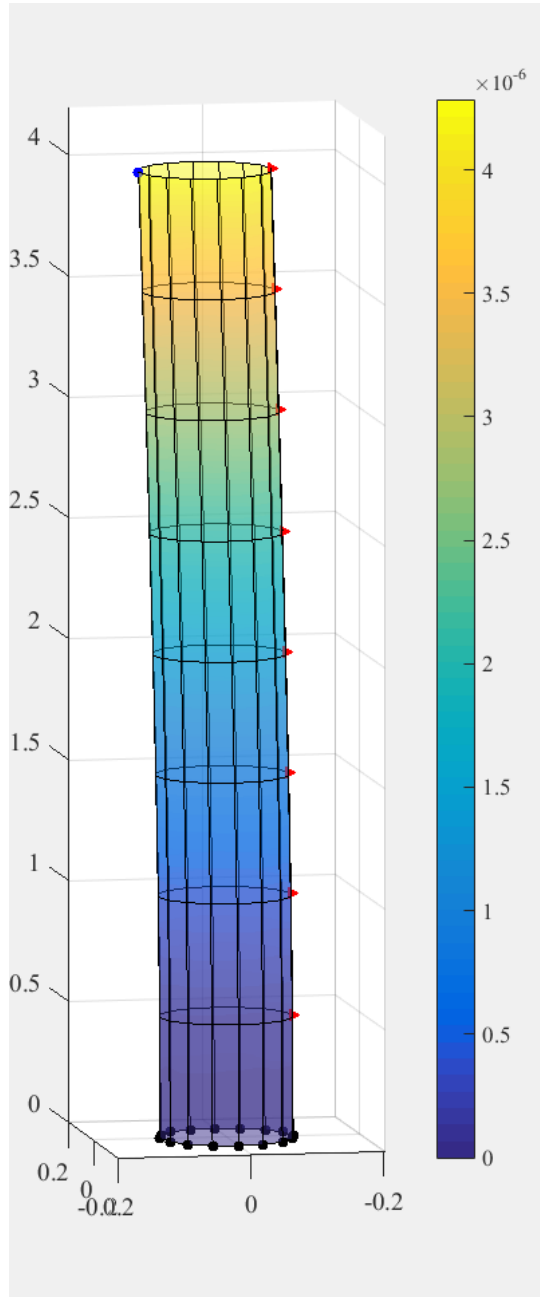
Figure 14 Contour of the displacement variance along the whole model due to 10% uncertianty
in the mass density at t=4.8s